

# Low-Temperature Hydrogen Production by Highly Efficient Catalytic System Assisted by an Electric Field<sup>†</sup>

Yasushi Sekine,\* Masayuki Haraguchi, Masahiko Tomioka, Masahiko Matsukata, and Eiichi Kikuchi

Department of Applied Chemistry, Waseda University, 3-4-1, Okubo, Shinjuku, Tokyo, 169-8555 Japan

Received: June 30, 2009; Revised Manuscript Received: August 23, 2009

We investigated four catalytic reactions assisted with an electric field to promote catalytic activity, and we could achieve an effective process for hydrogen production at low temperatures, such as 423 K. In the presence of the electric field, four reactions of steam reforming of ethanol, decomposition of ethanol, water gas shift, and steam reforming of methane proceeded at very low temperature, such as 423 K, where a conventional catalytic reaction hardly proceeded. Conversion of reactant was greatly increased by the electric field, and apparent activation energies for these four reactions were lowered by the application of the electric field. This process can produce hydrogen and syngas by using a considerably small energy demand and has quick response.

## 1. Introduction

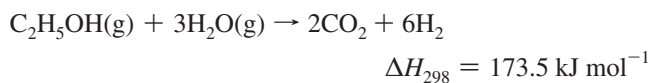
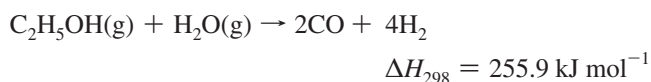
Hydrogen production from various energy sources such as fossil fuel and biomass is desired in the near future. Today, a major route for hydrogen production is catalytic steam reforming of methane, other hydrocarbons, or ethanol. The reaction is highly endothermic and requires a high temperature. As for high-temperature catalytic processes, there are many problems, such as selection of strong materials to heat, deactivation of the catalyst, and the difficulty of using wasted heat at a low temperature after the heat exchanger. The heat loss is a one of the reasons for the depression of the total energy efficiency of chemical processes. In the case of small commercial chemical processes without a heat exchanger, application of high temperature is a serious problem because of the high heat loss, so a low temperature catalytic process that works at a lower temperature without a heat exchanger is desirable for high energy efficiency.

To solve such problems, many researchers have investigated hybridization of nonequilibrium plasma and catalysts as novel chemical processes.<sup>1–14</sup> In addition, there have been many investigations for the utilization of electric power to convert such fuels into hydrogen/syngas.<sup>15–19</sup> In contrast, we have investigated catalytic reactions in an electric field. Since an electric field needs less energy than a nonequilibrium electrical discharge, the reaction can be conducted under milder conditions. We have reported the effect of an electric field on the catalytic decomposition of ethanol.<sup>20</sup> The reaction proceeds at a lower temperature region in which conventional catalytic reaction cannot take place. The electric field is not plasma, is milder than plasma, and has properties of lower consumption energy and no emission spectra.

In this research, we investigated steam reforming of ethanol and another three elemental reactions: ethanol decomposition, water gas shift reaction, and steam reforming of methane.

Ethanol is being paid a lot of attention as an alternative fuel. It can be easily produced by fermentation of carbohydrate of biomass, so ethanol is expected to be a clean energy source having many possibilities. In addition, development of effective use of ethanol as a fuel is important because petroleum will be in short supply in the future.

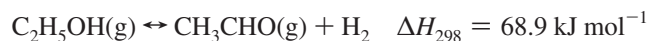
Steam reforming of ethanol is an endothermic reaction and requires high temperature, about 773 K or higher.



If this reaction could proceed at low temperature using wasted heat, a novel process for effective hydrogen production would be realized.

Many researches have investigated steam reforming of ethanol at the lower temperature region.<sup>21–41</sup> Supported Co catalyst exhibited high activity for steam reforming of ethanol,<sup>21</sup> and noble metals such as Pt, Pd, Rh, and Ru have shown high catalytic activities at 573–723 K.<sup>28,32,33</sup> We also investigated this steam reforming reaction over Co supported catalyst on perovskite oxide, such as SrTiO<sub>3</sub>,<sup>39,40</sup> and we found that the reaction mechanism for steam reforming of ethanol was a combination of the following five reactions:

(1) dehydrogenation of ethanol to form acetaldehyde,



$$\Delta G_{573} = -4.2 \text{ kJ mol}^{-1}, K_{p573} = 6.4 \times 10^3, \Delta G_{673} = -19.8 \text{ kJ mol}^{-1}, K_{p673} = 2.8 \times 10^6$$

(2a) steam reforming of acetaldehyde to form carbon monoxide and hydrogen,

<sup>†</sup> Part of the special issue “Green Chemistry in Energy Production Symposium”.

\* Corresponding author. Phone and Fax: +81-3-5286-3114. E-mail: ysekine@waseda.jp.



$$\Delta H_{298} = 186.9 \text{ kJ mol}^{-1}$$

(2b) decomposition of acetaldehyde to form methane and carbon monoxide,

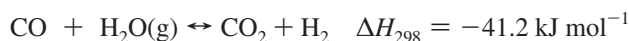


(3) steam reforming of methane,



$$\Delta G_{573} = 18.9 \text{ kJ mol}^{-1}, K_{p573} = 6.5 \times 10^{-8}, \Delta G_{673} = 13.0 \text{ kJ mol}^{-1}, K_{p673} = 5.9 \times 10^{-5}$$

(4) and water gas shift of carbon monoxide to carbon dioxide.



$$\Delta G_{573} = -4.2 \text{ kJ mol}^{-1}, K_{p573} = 3.9 \times 10,$$

$$\Delta G_{673} = 3.3 \text{ kJ mol}^{-1}, K_{p673} = 1.2 \times 10$$

In these sequential reactions, reaction 3, steam reforming of methane, is a highly endothermic reaction, so a high temperature is required. For this reaction, the Gibbs free energy at 573 K is positive, 18.9 kJ/mol; 13.0 kJ/mol at 673 K. As a result, the thermodynamic equilibrium constant for this reaction is only  $6.5 \times 10^{-8}$  at 573 K,  $5.9 \times 10^{-5}$  at 673 K. Although many researchers have investigated steam reforming of methane,<sup>42–54</sup> it is still a difficult problem to achieve a lower reaction temperature, higher conversion, and lower carbon deposits on the catalyst. On the other hand, reaction 4, a water gas shift reaction, is an exothermic reaction, but a conventional catalyst for the reaction, such as Cu/ZnO/Al<sub>2</sub>O<sub>3</sub> or Pt/CeO<sub>2</sub>, is not so highly active, not stable.<sup>55–75</sup>

In this research, we investigated steam reforming of ethanol, and we also conducted three reactions of ethanol decomposition, water gas shift reaction, and steam reforming of methane. In each reaction, a conventional catalytic reaction (mode A) and catalytic reaction in an electric field (mode B: named “*electreforming*”) were conducted and compared. Schematic images of the reaction systems in this research are shown in Figure 1.

## 2. Experimental Section

In previous research, we have found that noble metals such as Pt showed highly catalytic performance for steam reforming of ethanol. We choose Pt, Rh, and Pd as the supported metals for comparison in this research. We choose CeO<sub>2</sub> as the best catalyst support from previous investigations. CeO<sub>2</sub> shows a highly synergetic effect with an electric field,<sup>20</sup> so we prepared the following catalysts of 1 wt % Pt/CeO<sub>2</sub>, 1 wt % Pd/CeO<sub>2</sub>, and 1 wt % Rh/CeO<sub>2</sub>. The catalysts were prepared by an impregnation method. CeO<sub>2</sub> was soaked in distilled water and stirred and deaerated for 2 h at room temperature. An aqueous solution of the precursor of the supported metals (Pt(NH<sub>3</sub>)<sub>4</sub>(NO<sub>3</sub>)<sub>2</sub>, Pd(OCOCH<sub>3</sub>)<sub>2</sub>, Rh(NO<sub>3</sub>)<sub>3</sub>) was added, stirred for 2 h, evaporated to dryness, then calcined at 973 K and crushed into particles with sizes of 355–500 μm.

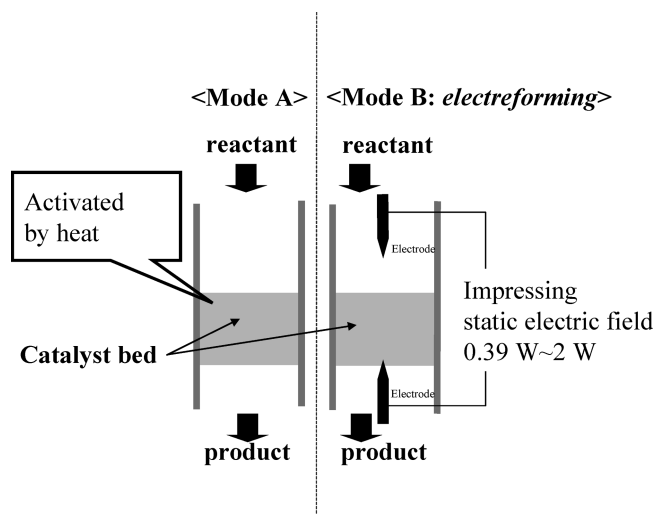


**Figure 1.** Schematic images for two catalytic reaction modes with/without an electric field.

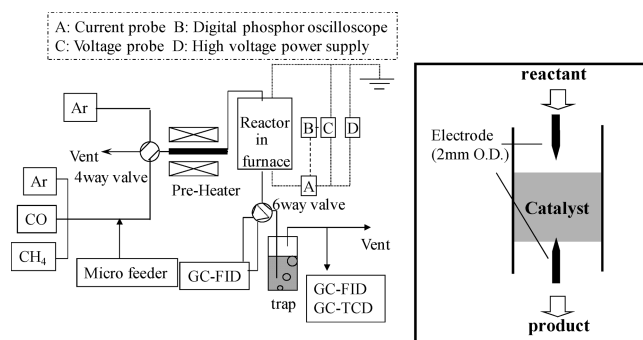


**Figure 2.** Reaction apparatus.

In all experiments, a quartz tube (6.0 mm o.d.) was used as a flow-type reactor, as shown in Figure 2. Two stainless steel rods (2.0 mm o.d.) were inserted from each end of the quartz tube as electrodes. In each reaction, reactant was supplied at a rate of 0.5 mmol min<sup>-1</sup>. Steam by carbon ratio was 2. In the cases of both mode A and mode B, 100 mg of catalyst was charged into the quartz reactor. The height of the catalyst bed was 4 mm, and the gap distance of each electrode was 5 mm, so the catalyst bed did not contact the tip of the upper electrode. The catalyst was pretreated in situ in a 5% hydrogen flow (Ar balance) at 723 or 823 K before the reaction to reduce the catalyst. Liquid reactants such as ethanol and water were supplied using a microfeeder (0.5 mmol min<sup>-1</sup>), evaporated in a preheating zone (423 K), and carried into the reactor through a gas line (393 K) with Ar (20 cc min<sup>-1</sup>). After the reaction, product gases were analyzed using a GC-FID and a GC-TCD after passing a cold trap (2-butanol). Liquid products were analyzed using a GC-FID before passing a cold trap. In this research, the conversion of reactant was calculated from product gases such as CO, CH<sub>4</sub>, CO<sub>2</sub>, C<sub>2</sub>H<sub>4</sub>, C<sub>2</sub>H<sub>6</sub>, and CH<sub>3</sub>CHO in each reaction.

$$\text{conversion (\%)} = \frac{\text{output moles of carbon atom in product gases}}{\text{input moles of carbon atom in reactant}} \times 100$$

The yield of each product without hydrogen was defined as below:

$$\text{yield (\%)} = \frac{\text{carbon moles of product species}}{\text{input moles of reactant}} \times 100$$

The yield of hydrogen was defined as below:

$$\text{H}_2 \text{ yield (\%)} = \frac{\text{moles of hydrogen}}{\text{input moles of reactant}} \times 100$$

A DC high-voltage power supply was used to generate the electric field. The electric field was controlled by input current with a fixed value of 3 mA, so the impressed voltage depended on the nature of the catalyst. Waveforms of the current and voltage were observed by a digital signal oscilloscope (Tektronix TDS3052B). The profile was flat for the voltage, and micro-pulse-shaped for the current. The applied electric pressure (voltage) was about 130–600 V, depending on the reactant and catalysts. The total input power was about 0.4–2 W.

### 3. Results and Discussion

**3.1. Steam Reforming of Ethanol.** First of all, we conducted steam reforming of ethanol over various catalysts with/without the electric field. Figure 3 shows the conversion of ethanol at 423–523 K by catalytic reaction without the electric field (mode A) and by catalytic reaction in the electric field (mode B: electroforming). Figure 4 shows the yield of products over each catalyst and in each reaction mode. From Figure 3, mode A shows low conversion for all catalysts about 10% or lower at 523 K, and conversion increased with an increase of reaction temperature. In mode B: electroforming, conversion was greatly increased for all catalysts by impressing the electric field to the catalyst bed. In the case of Pd/CeO<sub>2</sub> and Rh/CeO<sub>2</sub>, conversion was about 60% at 423 K that conventional catalytic steam reforming hardly proceeded, and maximum conversion of ethanol was 70.2% at 523 K over Pd/CeO<sub>2</sub> catalyst. In the case of Pt/CeO<sub>2</sub> catalyst, conversion was lower than the other two catalysts, and the maximum conversion of ethanol was 61.6% at 523 K. For the required reaction temperature to obtain the same conversion level between modes A and B, the application of the electric field can decrease the reaction temperature about 150 K or more for all catalysts.

Figure 4 indicates the effect of the electric field on the product distribution. In general, the reaction path of catalytic steam reforming of ethanol without the electric field is known as described above. Dehydrogenation of ethanol and formation of acetaldehyde and hydrogen is observed at very low conversion (initial step of the reaction). Sequential decomposition of acetaldehyde or steam reforming of acetaldehyde proceeds, and CO, CH<sub>4</sub> and H<sub>2</sub> are produced on the catalyst. Then CO reacts with water as a water gas shift (WGS) reaction, and CO<sub>2</sub> and H<sub>2</sub> are produced.

As characteristic parameters for this reaction, we examined the ratio of  $r_R/r_D$  and the WGS ratio, which are defined as follows;

$$r_R/r_D(-) = \frac{f(\text{CO}) + f(\text{CO}_2) - f(\text{CH}_4)}{f(\text{CH}_4)}$$

$$\text{WGS ratio (\%)} = \frac{f(\text{CO}_2)}{f(\text{CO}) + f(\text{CO}_2)} \times 100$$

In the formula,  $f(\text{product})$  means formation rate of each product. The parameter of  $r_R/r_D$  represents the ratio of the

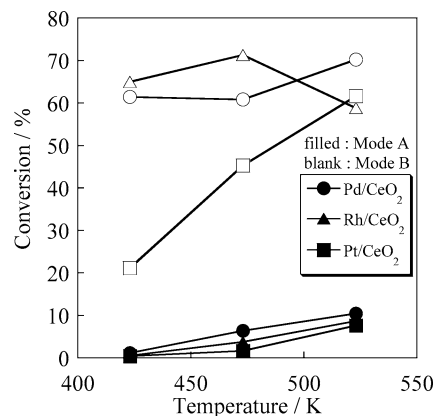


**Figure 3.** Effect of temperature on the conversion of catalytic steam reforming of ethanol without the electric field (mode A) and with the electric field (mode B: electroforming).

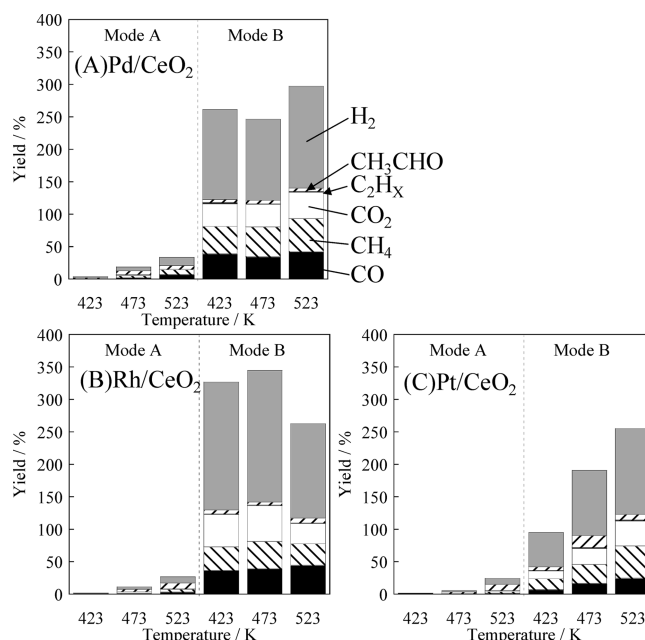


**Figure 4.** Effect of temperature on the yield of products for catalytic steam reforming of ethanol without the electric field (mode A) and with the electric field (mode B: electroforming).

reaction rate of steam reforming and the decomposition of acetaldehyde. If the steam reforming of acetaldehyde is the dominant reaction over decomposition of it, the value of  $r_R/r_D$  would become larger. The WGS ratio means the reactivity for the WGS reaction on this condition. Notice that these parameters are calculated supposing CO and CH<sub>4</sub> are generated from only reactions of steam reforming or decomposition of acetaldehyde, and no methanation has been considered. This assumption was based on the experimental result in which we could not observe the formation of methane by steam reforming of “methanol” with the same catalyst at the same temperature (results are not shown), and CO<sub>2</sub> is assumed to be generated only by the WGS reaction.

Table 1 shows the ratio of  $r_R/r_D$  and WGS for each catalyst and in each reaction mode. In mode A with Pd/CeO<sub>2</sub> or Pt/CeO<sub>2</sub> catalyst, steam reforming of acetaldehyde slightly proceeded, and decomposition of acetaldehyde was a dominant reaction because the  $r_R/r_D$  ratio was almost 0. Over Rh/CeO<sub>2</sub> catalyst, these two reactions proceeded simultaneously because  $r_R/r_D$  ratio was about 0.2–0.3. Over Pd/CeO<sub>2</sub> or Rh/CeO<sub>2</sub> catalyst, WGS ratio was about 10–30%, and over Pt/CeO<sub>2</sub>

**TABLE 1: Steam-Reforming/Decomposition Ratio and Water Gas Shift Ratio over Three Catalysts with/without EF (electric field) on Steam Reforming of Ethanol**

	temp, K	Pd/CeO <sub>2</sub>		Rh/CeO <sub>2</sub>		Pt/CeO <sub>2</sub>	
		$r_R/r_D$ , -	WGS ratio, %	$r_R/r_D$ , -	WGS ratio, %	$r_R/r_D$ , -	WGS ratio, %
mode A (without EF)	523	0.01	8.2	0.34	21.2	0.07	42.9
mode B, electroreforming	423	0.74	47.4	1.39	57.9	0.13	62.9
with EF	473	0.50	50.6	1.27	58.3	0.38	60.2
	523	0.62	49.0	1.31	41.1	0.28	61.0

**TABLE 2: Reaction Enthalpy and Energy Gain for the Steam Reforming of Ethanol over Three Catalysts with/without the Electric Field at Each Temperature**

temp, K	catalyst with/ without EF	conversion, %	formation rate (C-base)/ $\mu\text{mol min}^{-1}$						$\sum \Delta H_{c-P}^a$ , J min <sup>-1</sup>	$\Delta H_{c-EtOH}^b$ , J min <sup>-1</sup>	$\Delta H_r^c$ , J min <sup>-1</sup>	$\Delta E_{ef}^d$ , J min <sup>-1</sup>
			H <sub>2</sub>	CH <sub>3</sub> CHO	C <sub>2</sub>	CO <sub>2</sub>	CH <sub>4</sub>	CO				
423	Pd/CeO <sub>2</sub>	1.1	8.3	8.6	0.0	0.1	0.8	0.5	13.5	8.0	5.4	
	Pd/CeO <sub>2</sub> with EF	61.4	691.4	22.9	10.8	87.3	105.7	97.1	362.7	432.7	-70.0	-75.4
	Rh/CeO <sub>2</sub>	0.5	4.6	3.7	0.0	0.1	0.3	0.3	6.1	3.6	2.5	
	Rh/CeO <sub>2</sub> with EF	65.0	986.0	28.5	3.8	125.6	90.8	91.4	428.3	457.8	-29.5	-32.0
	Pt/CeO <sub>2</sub>	0.4	4.0	3.1	0.0	0.2	0.1	0.0	4.9	2.6	2.3	
473	Pt/CeO <sub>2</sub> with EF	21.1	262.6	29.3	1.9	30.0	42.1	17.7	155.3	148.7	6.6	4.4
	Pd/CeO <sub>2</sub>	6.4	29.7	28.7	0.0	4.5	7.3	5.8	50.8	45.0	5.8	
	Pd/CeO <sub>2</sub> with EF	60.8	624.2	28.7	1.5	87.6	115.7	85.5	342.1	428.3	-86.2	-92.1
	Rh/CeO <sub>2</sub>	3.7	18.5	16.2	0.0	5.7	2.7	2.2	27.6	26.3	1.3	
	Rh/CeO <sub>2</sub> with EF	71.2	1012.4	23.1	4.1	138.2	104.5	98.8	444.1	502.0	-57.8	-59.1
523	Pt/CeO <sub>2</sub>	1.6	10.4	13.2	0.0	0.4	0.8	0.4	19.5	11.6	8.0	
	Pt/CeO <sub>2</sub> with EF	45.2	502.0	91.8	6.2	61.6	74.4	40.7	340.1	318.7	21.4	13.4
	Pd/CeO <sub>2</sub>	10.4	63.6	28.3	0.3	1.6	18.8	17.4	74.0	73.4	0.6	
	Pd/CeO <sub>2</sub> with EF	70.2	784.6	25.6	6.9	101.3	127.7	105.6	408.9	494.7	-85.9	-86.5
	Rh/CeO <sub>2</sub>	8.7	46.9	44.2	0.1	2.6	9.0	9.5	77.0	61.0	16.0	
	Rh/CeO <sub>2</sub> with EF	58.8	726.5	38.8	1.8	78.4	82.6	112.2	361.9	414.2	-52.3	-68.3
	Pt/CeO <sub>2</sub>	7.6	45.6	48.7	0.0	3.0	6.6	4.0	78.1	53.6	24.6	
	Pt/CeO <sub>2</sub> with EF	61.6	660.6	44.1	6.7	96.8	123.6	61.7	378.9	434.0	-55.0	-79.6

<sup>a</sup>  $\sum \Delta H_{c-P}$ : summation of standard combustion enthalpy of products. <sup>b</sup>  $\Delta H_{c-EtOH}$ : summation of standard combustion enthalpy of consumed ethanol. <sup>c</sup>  $\Delta H_r$ : endothermic enthalpy of the reaction. <sup>d</sup>  $\Delta E_{ef}$ : the difference of  $\Delta H_r$  (without the electric field) and  $\Delta H_r$  (with the electric field) at the same temperature.

catalyst, the WGS ratio was about 50%. In mode B,  $r_R/r_D$  and the WGS ratio were increased over all the catalysts by the application of the electric field. Especially on the Rh/CeO<sub>2</sub> catalyst,  $r_R/r_D$  greatly increased up to 1.3. It was supposed that the reason for the increase in  $r_R/r_D$  was the shift of the reaction path from decomposition of acetaldehyde to steam reforming of acetaldehyde or promotion of steam reforming of methane, which was generated by the decomposition of acetaldehyde. The WGS ratio also increased up to 50–60% for all catalysts by the application of the electric field. Thus, by impressing of the electric field, hydrogen production was promoted by the change of the reaction path.

Table 2 shows the formation rate of products; their combustion enthalpy; and the endothermic enthalpy gain,  $\Delta E_{ef}$ . The respective energies were about from 13.4 J/min (endothermic) to -92.1 J/min (exothermic) for the catalysts Rh, Pd, and Pt/CeO<sub>2</sub>. The input electric energy at 473 K was 72.4 J/min (= 1.21 W; Pd/CeO<sub>2</sub>), 98.2 J/min (= 1.64 W; Rh/CeO<sub>2</sub>), and 92.0 J/min (= 1.53 W; Pt/CeO<sub>2</sub>), respectively. Although the synergistic effect of noble metal and CeO<sub>2</sub> support with the electric field was observed, electric energy was consumed as heat, and the reactant ethanol lost a part of its calorific value by exothermic reaction in the cases of Pd or Rh catalysts.

**3.2. Decomposition of Ethanol.** Next, we examined decomposition of ethanol over various catalysts to investigate the role of steam in the electric field.

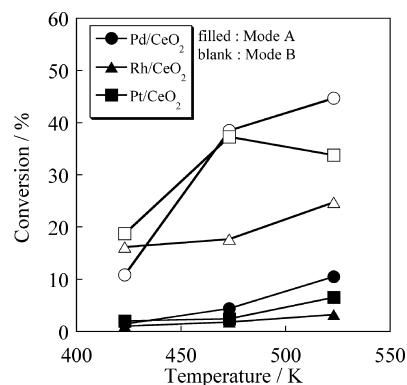
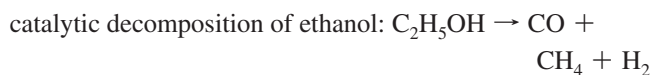


**Figure 5.** Effect of temperature on the conversion of catalytic decomposition of ethanol without the electric field (mode A) and with the electric field (mode B: electroreforming).

Figure 5 shows the conversion of ethanol for the catalytic decomposition of ethanol without the electric field (mode A) and for the catalytic decomposition of ethanol in the electric field (mode B: electroreforming). Figure 6 shows the yield of products over each catalyst and in each reaction mode. In Figure 5, the conversion of ethanol was increased for all catalysts by impressing the electric field to the catalyst bed. The rate of conversion was in the following order: Pd/CeO<sub>2</sub> > Rh/CeO<sub>2</sub> > Pt/CeO<sub>2</sub>. The promotion effect was smaller than that of steam reforming of ethanol. It seems that the existence of steam in the reaction field promoted synergistic interaction between the catalyst and the electric field. In Figure 6, the effect of the electric field on catalytic decomposition of ethanol (mode A)

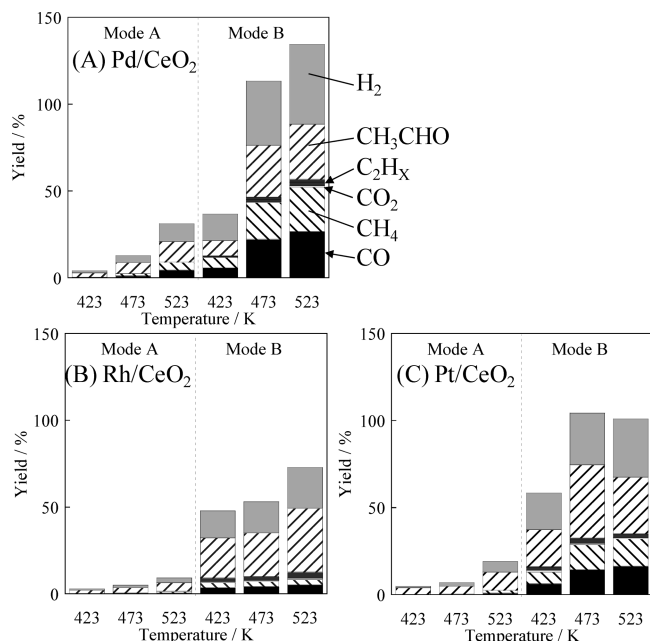


**Figure 6.** Effect of temperature on the yield of products for catalytic decomposition of ethanol without the electric field (mode A) and with the electric field (mode B: electroforming).

was examined. Over Pt/CeO<sub>2</sub> or Pd/CeO<sub>2</sub> catalyst, dehydrogenation of ethanol produced acetaldehyde, and its sequential decomposition to CO and CH<sub>4</sub> was observed. In the case of electroforming, selectivity to products did not change so much, but a small amount of ethylene formation was observed. Over the Rh/CeO<sub>2</sub> catalyst, ethanol was only dehydrogenated, and acetaldehyde was generated. Decomposition of acetaldehyde hardly proceeded in mode A. During electroforming, simultaneous reaction of dehydrogenation and dehydration of ethanol proceeded to acetaldehyde, ethylene, H<sub>2</sub>, and H<sub>2</sub>O. Sequential steam reforming of acetaldehyde and the WGS reaction were also promoted over this catalyst to produce H<sub>2</sub>O, CO, H<sub>2</sub>, and CO<sub>2</sub> by the electric field.

Table 3 presents the effects of an electric field on the catalytic decomposition of ethanol over various catalysts. On the basis of these results, the synergetic effect of a noble metal and CeO<sub>2</sub> with the electric field is extremely high, especially for Rh/CeO<sub>2</sub> catalyst. Regarding the endothermic enthalpy gain  $\Delta E_{\text{ef}}$ , the respective energies were 13.5–26.3 J/min for Pd/CeO<sub>2</sub> catalyst, 64.9–102.7 J/min for Rh/CeO<sub>2</sub> catalyst, and 38.3–81.7 J/min for Pt/CeO<sub>2</sub> catalyst. On the other hand, the input electric energy at 473 K was 55.8 J/min (= 0.93 W; Pd/CeO<sub>2</sub>), 87.3 J/min (= 1.46 W; Rh/CeO<sub>2</sub>), and 39.7 J/min (= 0.66 W; Pt/CeO<sub>2</sub>). Consequently, almost all the electric energy injection was used for the endothermic reaction.

**3.3. WGS Reaction.** As for the investigation of the reaction of steam reforming of ethanol in section 3.1, the WGS reaction was promoted by impressing the electric field, so the water gas shift reaction in the electric field was conducted using CO as a reactant to investigate the effect of the electric field. The WGS reaction is an exothermic reaction, as shown in following equation:



The reaction is desired to proceed at lower temperature by the thermodynamic equilibrium limitation due to its exothermic

reaction. On the other hand, the reaction rate is very small at lower temperature by kinetics limitation.

Figure 7 shows the conversion of CO in each reaction mode. Figure 8 shows the yield of products over each catalyst and in each reaction mode. In Figure 7, it can be seen that conversion was greatly increased at all temperatures by impressing the electric field. Especially over Rh/CeO<sub>2</sub> catalyst, the effect of the electric field was very large.

In Figure 8, it can be seen that for all catalysts and reaction modes, CO<sub>2</sub> and H<sub>2</sub> were mainly generated, and the formation ratio of CO<sub>2</sub> and H<sub>2</sub> was almost 1:1, so disproportionation of CO was negligible under this condition. A trace amount of ethylene and CH<sub>4</sub> was generated by impressing the electric field. Using Rh/CeO<sub>2</sub>, the yield of methane was about 2% in mode B. These phenomena suggest that the electric field promoted methane formation by changing the reaction path or enhancing the catalytic activity of methanation. Table 4 presents the effect of the electric field on the water gas shift reaction over various catalysts. Regarding the endothermic enthalpy gain,  $\Delta E_{\text{ef}}$ , the respective energies were 1.8–18.8 J/min for Pd/CeO<sub>2</sub>, 6.0–8.2 J/min for Rh/CeO<sub>2</sub>, and –1.3 to 6.7 J/min for Pd/CeO<sub>2</sub> catalyst. The input electric energy at 473 K was 120.3 J/min (= 2.00 W; Pd/CeO<sub>2</sub>), 105.7 J/min (= 1.76 W; Rh/CeO<sub>2</sub>), and 78.8 J/min (= 1.31 W; Pt/CeO<sub>2</sub>). Consequently, almost all the electric energy injection was used for the activation of the reactant.

**3.4. Steam Reforming of Methane.** Steam reforming of methane in the electric field was also conducted to investigate the possibility of steam reforming of methane that was generated from decomposition of acetaldehyde or methanation.

So far, conventional catalytic steam reforming of methane has been operated at high temperatures, such as 1000 K. Since the thermodynamic equilibrium constant of the reaction was quite small at low temperatures such as 423–523 K, catalytic steam reforming of methane with wasted heat hardly proceeds under such low temperature conditions without an electric field.

Figure 9 shows conversion of methane over each catalyst and in each reaction mode. Figure 10 shows the yield of products over each catalyst and in each reaction mode. In Figure 9, mode A shows little or no activity at 423–573 K. On electroforming, steam reforming of methane proceeded, but conversion was lower than other reactions in this research. The effect of the electric field was comparatively large when using the Rh/CeO<sub>2</sub> catalyst. Conversion of methane was increased by increasing the input current. In Figure 10, it is shown that CO<sub>2</sub> and H<sub>2</sub> were mainly generated in mode B. Thus, the WGS reaction proceeded over all catalysts, and over Rh/CeO<sub>2</sub> catalyst, CO formation was comparatively greater than over the other two catalysts.

Table 5 shows the effect of the electric field on steam reforming of methane over various catalysts. Regarding the endothermic enthalpy gain,  $\Delta E_{\text{ef}}$ , the energies were 18.8–26.1 J/min for the Pd/CeO<sub>2</sub> catalyst, 38.0–43.2 J/min for the Rh/CeO<sub>2</sub> catalyst, and 19.2–32.8 J/min for Pt/CeO<sub>2</sub> catalyst. The input electric energy was 79.5 J/min (= 1.32 W; Pd/CeO<sub>2</sub>), 166.5 J/min (= 2.78 W; Rh/CeO<sub>2</sub>), and 167.9 J/min (= 2.80 W; Pt/CeO<sub>2</sub>). Consequently, about 25% of the electric energy injection was used for the endothermic reaction. Optimizing the reaction conditions would lessen the energy demand. From these results, the synergetic effect of a noble metal and CeO<sub>2</sub> with the electric field is extremely high for this reaction.

**3.5. Mechanism of Promotion Effect on the electroforming.** From the experimental results above, we considered the promoting mechanism of electroforming from kinetics and thermodynamics. First, we estimated the apparent activation

**TABLE 3: Reaction Enthalpy and Energy Gain for the Decomposition of Ethanol over Three Catalysts with/without the Electric Field at Each Temperature**

temp, K	catalyst with/ without EF	conversion, %	formation rate (C-base), $\mu\text{mol min}^{-1}$						$\sum\Delta H_{c-P}^a$ , J $\text{min}^{-1}$	$\Delta H_{c-EtOH}^b$ , J $\text{min}^{-1}$	$\Delta H_r^c$ , J $\text{min}^{-1}$	$\Delta E_{ef}^d$ , J $\text{min}^{-1}$
			H <sub>2</sub>	CH <sub>3</sub> CHO	C <sub>2</sub>	CO <sub>2</sub>	CH <sub>4</sub>	CO				
423	Pd/CeO <sub>2</sub>	1.4	6.2	12.5	0.0	0.0	0.5	0.4	17.2	10.1	7.2	
	Pd/CeO <sub>2</sub> with EF	10.8	76.4	42.4	5.0	0.5	14.3	15.1	96.9	76.2	20.7	13.5
	Rh/CeO <sub>2</sub>	1.0	4.1	9.3	0.0	0.1	0.2	0.2	12.5	7.3	5.2	
	Rh/CeO <sub>2</sub> with EF	16.2	78.0	115.2	10.7	1.6	6.7	9.2	184.2	114.1	70.1	64.9
	Pt/CeO <sub>2</sub>	2.0	4.6	19.4	0.0	0.0	0.2	0.1	24.6	14.1	10.5	
473	Pt/CeO <sub>2</sub> with EF	18.7	105.3	106.5	10.3	2.4	16.9	15.9	192.1	131.9	60.2	49.7
	Pd/CeO <sub>2</sub>	4.4	20.0	31.4	0.0	0.1	3.3	3.0	46.9	31.1	15.7	
	Pd/CeO <sub>2</sub> with EF	38.5	184.2	149.3	13.1	1.1	52.9	55.7	313.2	271.2	42.0	26.3
	Rh/CeO <sub>2</sub>	1.8	6.8	14.6	0.0	0.1	0.8	0.8	20.3	12.7	7.6	
	Rh/CeO <sub>2</sub> with EF	17.7	89.5	125.9	11.6	1.3	7.3	10.5	202.6	124.5	78.1	70.5
523	Pt/CeO <sub>2</sub>	2.4	10.4	22.4	0.0	0.1	0.6	0.4	30.3	17.2	13.1	
	Pt/CeO <sub>2</sub> with EF	37.3	148.6	209.6	15.6	2.0	35.5	36.4	357.7	262.8	94.9	81.7
	Pd/CeO <sub>2</sub>	10.5	51.2	59.6	0.1	0.1	11.1	11.3	99.0	74.0	25.0	
	Pd/CeO <sub>2</sub> with EF	44.7	229.9	157.9	19.3	2.1	63.6	66.9	358.5	314.7	43.8	18.7
	Rh/CeO <sub>2</sub>	3.2	13.5	24.8	0.1	0.2	1.6	1.7	35.5	22.6	12.9	
	Rh/CeO <sub>2</sub> with EF	24.7	117.7	183.1	18.4	2.0	7.4	13.1	289.9	174.3	115.6	102.7
	Pt/CeO <sub>2</sub>	6.5	29.6	52.2	0.3	0.1	3.6	2.7	75.1	46.0	29.1	
	Pt/CeO <sub>2</sub> with EF	33.8	167.4	161.7	11.8	1.4	39.7	40.8	305.3	237.8	67.4	38.3

<sup>a</sup>  $\sum\Delta H_{c-P}$ : summation of standard combustion enthalpy of products. <sup>b</sup>  $\Delta H_{c-EtOH}$ : summation of standard combustion enthalpy of consumed ethanol. <sup>c</sup>  $\Delta H_r$ : endothermic enthalpy of the reaction. <sup>d</sup>  $\Delta E_{ef}$ : the difference of  $\Delta H_r$  (without the electric field) and  $\Delta H_r$  (with the electric field) at the same temperature.

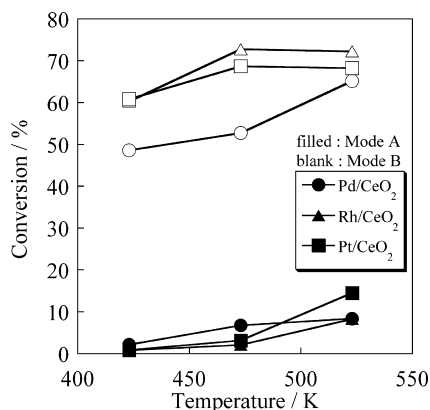


**Figure 7.** Effect of temperature on the conversion of water gas shift reaction without the electric field (mode A) and with the electric field (mode B: electroforming).

energy for these four reactions over the three catalysts. We assumed that all the reactions were pseudo-first-order reactions in the reactant concentration, and zero-order in the water concentration for steam reforming of ethanol, water gas shift reaction, and steam reforming of methane. Apparent activation energies were calculated by following the Arrhenius equation.

$$\ln k = \ln A - E_a/RT$$

where  $A$  is the preexponential frequency factor,  $E_a$  is the apparent activation energy and  $R = 8.314 \text{ J/mol/K}$ .

Table 6 shows the apparent activation energies for four reactions on the three catalysts with/without the electric field (EF), and Table 7 shows the preexponential frequency factors for the same, calculated by the Arrhenius equation. From these calculated results, application of the electric field for the catalyst bed lowered the apparent activation energy for all four reactions. This phenomenon might be derived from the activation of the catalyst by the positive effect of the charge of an electron on the active metals due to the dielectric polarization by electre-

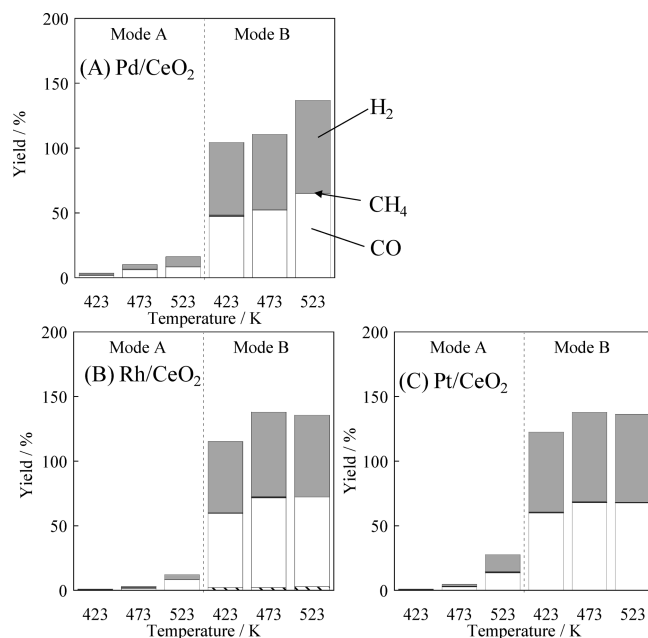


**Figure 8.** Effect of temperature on the yield of products for water gas shift reaction without the electric field (mode A) and with the electric field (mode B: electroforming).

forming. As for the preexponential frequency factor, although the value was not changed much on the decomposition (DC) of ethanol and water gas shift reaction, the value decreased much on the steam reforming (SR) of ethanol or methane. The preexponential frequency factor  $A$  is described as follows:

$$A = \sigma L(8kT/\pi\mu)^{1/2}$$

From this equation and these calculated results, it is seen that the electric field changes the mobility of molecules under the same temperature conditions. Further investigations would need to be conducted for the elucidation of the reaction mechanism of electroforming.

**TABLE 4: Reaction Enthalpy and Energy Gain for the Water Gas Shift Reaction over Three Catalysts with/without the Electric Field at Each Temperature**

temp, K	catalyst with/ without EF	conversion, %	formation rate (C-base), $\mu\text{mol min}^{-1}$				$\sum\Delta H_{c-P}^a$ , J $\text{min}^{-1}$	$\Delta H_{c-\text{reactant}}^b$ , J $\text{min}^{-1}$	$\Delta H_r^c$ , J $\text{min}^{-1}$	$\Delta E_{\text{ef}}^d$ , J $\text{min}^{-1}$
			H <sub>2</sub>	C <sub>2</sub>	CO <sub>2</sub>	CH <sub>4</sub>				
423	Pd/CeO <sub>2</sub>	2.1	7.0	1.1	9.5	0.0	3.6	3.0	0.6	
	Pd/CeO <sub>2</sub> with EF	48.6	278.4	5.7	237.1	0.0	88.1	68.7	19.4	18.8
	Rh/CeO <sub>2</sub>	0.8	1.0	1.1	2.9	0.0	2.0	1.1	0.8	
	Rh/CeO <sub>2</sub> with EF	60.2	274.7	3.0	287.9	10.2	92.1	85.2	6.9	6.0
	Pt/CeO <sub>2</sub>	0.8	0.6	2.3	1.9	0.0	3.6	1.2	2.4	
473	Pt/CeO <sub>2</sub> with EF	60.8	308.4	3.7	299.6	0.6	94.2	86.0	8.2	5.8
	Pd/CeO <sub>2</sub>	6.8	16.2	2.3	31.5	0.0	8.1	9.6	-1.4	
	Pd/CeO <sub>2</sub> with EF	52.7	289.1	2.3	260.9	0.5	86.5	74.6	11.9	13.3
	Rh/CeO <sub>2</sub>	2.1	4.7	2.1	8.3	0.0	4.5	2.9	1.5	
	Rh/CeO <sub>2</sub> with EF	72.7	326.1	5.8	346.2	11.5	112.2	102.9	9.3	7.8
523	Pt/CeO <sub>2</sub>	3.2	7.6	2.0	13.8	0.0	5.2	4.5	0.7	
	Pt/CeO <sub>2</sub> with EF	68.6	345.6	3.3	339.0	0.9	104.5	97.1	7.4	6.7
	Pd/CeO <sub>2</sub>	8.4	38.5	0.0	41.9	0.0	11.0	11.9	-0.8	
	Pd/CeO <sub>2</sub> with EF	65.1	325.6	0.0	325.6	0.0	93.1	92.1	0.9	1.8
	Rh/CeO <sub>2</sub>	8.3	19.1	0.0	41.4	0.0	5.5	11.7	-6.3	
	Rh/CeO <sub>2</sub> with EF	72.2	317.2	0.0	345.8	15.1	104.1	102.1	2.0	8.2
	Pt/CeO <sub>2</sub>	14.5	65.8	5.1	67.5	0.0	26.5	20.5	5.9	
	Pt/CeO <sub>2</sub> with EF	68.2	339.9	1.7	337.7	1.6	101.0	96.5	4.6	-1.3

<sup>a</sup>  $\sum\Delta H_{c-P}$ : summation of standard combustion enthalpy of products. <sup>b</sup>  $\Delta H_{c-\text{EIOH}}$ : summation of standard combustion enthalpy of consumed CO. <sup>c</sup>  $\Delta H_r$ : endothermic enthalpy of the reaction. <sup>d</sup>  $\Delta E_{\text{ef}}$ : the difference of  $\Delta H_r$  (without the electric field) and  $\Delta H_r$  (with the electric field) at the same temperature.

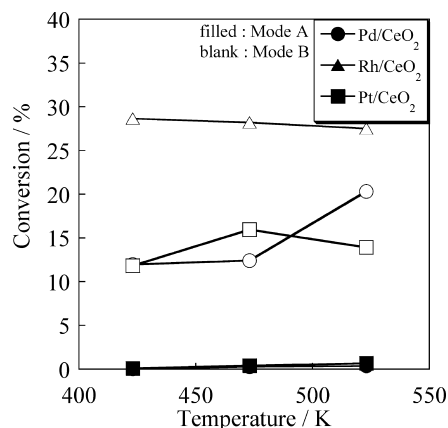


**Figure 9.** Effect of temperature on the conversion of catalytic steam reforming of methane without the electric field (mode A) and with the electric field (mode B: electroforming).

**3.6. Energy Efficiency of electroforming.** From these results, the electroforming enabled hydrogen production at a lower temperature. Table 8 shows the energy demand on each reaction/catalyst by electroforming to produce 1 kg of H<sub>2</sub>. Table 9 shows the energy demand to produce 1 kg of syngas (H<sub>2</sub> + CO) and the H<sub>2</sub>/CO ratio. In this calculation, the input energy was calculated from the energy demand to impress the electric field, and  $\Delta E_{\text{ef}}$  in Tables 2–5 shows the difference values of the energy consumption between conventional catalytic reactions and electroforming. In Table 8, it is seen that the energy demand of hydrogen production was 50–129 MJ/kg<sub>H<sub>2</sub></sub> by steam reforming of ethanol, 109–568 MJ/kg<sub>H<sub>2</sub></sub> by decomposition of ethanol, 114–208 MJ/kg<sub>H<sub>2</sub></sub> by WGS reaction, and 144–359 MJ/kg<sub>H<sub>2</sub></sub> by steam reforming of methane in these processes of electroforming. These energies depend on the kind of catalysts and reaction temperatures. Rh/CeO<sub>2</sub> and Pd/CeO<sub>2</sub> catalysts showed lower energy demands for hydrogen production by steam reforming of ethanol/methane, and Pt/CeO<sub>2</sub> was effective in the WGS reaction.

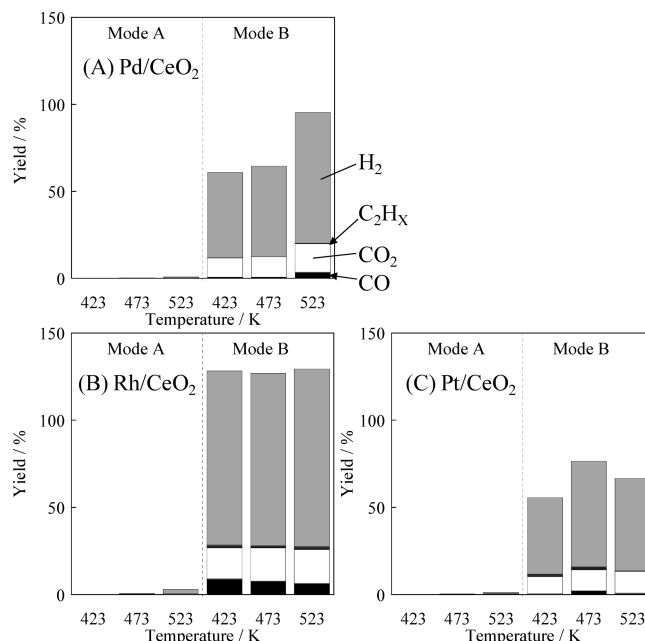


**Figure 10.** Effect of temperature on the yield of products for catalytic steam reforming of methane without the electric field (mode A) and with the electric field (mode B: electroforming).

In Table 9, for the steam reforming of ethanol, it is seen that the energy demand was about 12–45 MJ/kg<sub>syngas</sub> and the H<sub>2</sub>/CO ratio was about 3–5 on all catalysts. The energy demand for syngas production by ethanol decomposition was 12–44 MJ/kg<sub>syngas</sub> using Pt/CeO<sub>2</sub> and Pd/CeO<sub>2</sub> catalysts and 56–132 MJ/kg<sub>syngas</sub> over Rh/CeO<sub>2</sub> catalyst. The H<sub>2</sub>/CO ratio was about 2 over Pt/CeO<sub>2</sub> and Pd/CeO<sub>2</sub> and 4.2–4.5 over Rh/CeO<sub>2</sub>. The gas composition was hydrogen-rich because a small amount of acetaldehyde was not completely decomposed. For the steam reforming of methane, the energy demand was 63–307 MJ/kg<sub>syngas</sub>. The H<sub>2</sub>/CO ratio was quite large because the WGS reaction proceeded well on these catalysts. The energy demand might be smaller by optimizing the reaction conditions.

**TABLE 5: Reaction Enthalpy and Energy Gain for the Steam Reforming of Methane over Three Catalysts with/without the Electric Field at Each Temperature**

temp, K	catalyst with/ without EF	conversion, %	formation rate (C-base), $\mu\text{mol min}^{-1}$				$\sum\Delta H_{c-P}^a$ , J $\text{min}^{-1}$	$\Delta H_{c-\text{CH}_4}^b$ , J $\text{min}^{-1}$	$\Delta H_r^c$ , J $\text{min}^{-1}$	$\Delta E_{\text{ef}}^d$ , J $\text{min}^{-1}$
			H <sub>2</sub>	C <sub>2</sub>	CO <sub>2</sub>	CO				
423	Pd/CeO <sub>2</sub>	0.0	0.0	0.0	0.1	0.0	0.0	0.0	0.0	
	Pd/CeO <sub>2</sub> with EF	12.0	244.4	0.7	55.4	3.6	71.9	53.2	18.7	
	Rh/CeO <sub>2</sub>	0.0	0.0	0.0	0.0	0.0	0.0	0.0	0.0	
	Rh/CeO <sub>2</sub> with EF	28.6	498.3	9.1	88.7	45.4	168.9	127.5	41.4	
	Pt/CeO <sub>2</sub>	0.1	0.5	0.3	0.3	0.0	0.5	0.4	0.1	
473	Pt/CeO <sub>2</sub> with EF	11.8	219.2	6.8	49.7	2.7	73.6	52.6	21.0	
	Pd/CeO <sub>2</sub>	0.3	0.3	0.0	1.3	0.0	0.1	1.2	-1.1	
	Pd/CeO <sub>2</sub> with EF	12.4	260.8	0.2	58.2	3.6	75.9	55.2	20.7	
	Rh/CeO <sub>2</sub>	0.3	2.3	0.0	1.5	0.0	0.7	1.3	-0.6	
	Rh/CeO <sub>2</sub> with EF	28.2	494.2	7.0	94.9	39.1	162.8	125.5	37.4	
523	Pt/CeO <sub>2</sub>	0.4	0.5	0.2	1.8	0.0	0.4	1.7	-1.3	
	Pt/CeO <sub>2</sub> with EF	15.9	303.5	8.4	59.9	11.5	102.5	71.0	31.5	
	Pd/CeO <sub>2</sub>	0.4	2.3	0.1	1.7	0.0	0.8	1.6	-0.8	
	Pd/CeO <sub>2</sub> with EF	20.3	375.3	2.3	81.4	18.0	115.8	90.5	25.3	
	Rh/CeO <sub>2</sub>	0.6	12.3	0.0	3.2	0.0	3.5	2.8	0.7	
	Rh/CeO <sub>2</sub> with EF	27.5	509.3	7.8	97.4	32.4	166.4	122.4	43.9	
	Pt/CeO <sub>2</sub>	0.7	3.2	0.8	2.6	0.0	2.0	2.9	-0.9	
	Pt/CeO <sub>2</sub> with EF	13.9	263.6	2.4	62.5	4.8	80.2	61.9	18.3	

<sup>a</sup> $\sum\Delta H_{c-P}$ : summation of standard combustion enthalpy of products. <sup>b</sup> $\Delta H_{c-\text{EtOH}}$ : summation of standard combustion enthalpy of consumed methane. <sup>c</sup> $\Delta H_r$ : endothermic enthalpy of the reaction. <sup>d</sup> $\Delta E_{\text{ef}}$ : the difference of  $\Delta H_r$  (without the electric field) and  $\Delta H_r$  (with the electric field) at the same temperature.

**TABLE 6: Apparent Activation Energy for Four Reactions on the Three Catalysts with/without EF, Calculated from Arrhenius Plots**

apparent $E_a$ , kJ/mol	C <sub>2</sub> H <sub>5</sub> OH SR	C <sub>2</sub> H <sub>5</sub> OH DC	WGS	CH <sub>4</sub> SR
Pd/CeO <sub>2</sub>	42.2	37.6	26.4	67.1
Pd/CeO <sub>2</sub> with EF	4.2	30.9	8.3	10.3
Rh/CeO <sub>2</sub>	53.4	21.0	43.0	77.6
Rh/CeO <sub>2</sub> with EF		8.5	6.2	
Pt/CeO <sub>2</sub>	56.0	21.6	53.6	35.2
Pt/CeO <sub>2</sub> with EF	25.9	13.2	3.8	3.5

**TABLE 7: Preexponential Frequency Factor for Four Reactions on Three Catalysts with/without EF Calculated from Arrhenius Plots**

ln A	C <sub>2</sub> H <sub>5</sub> OH SR	C <sub>2</sub> H <sub>5</sub> OH DC	WGS	CH <sub>4</sub> SR
Pd/CeO <sub>2</sub>	17.3	16.0	13.4	19.9
Pd/CeO <sub>2</sub> with EF	10.7	16.4	11.5	10.4
Rh/CeO <sub>2</sub>	19.6	11.0	16.9	22.8
Rh/CeO <sub>2</sub> with EF	8.9	10.2	11.3	8.3
Pt/CeO <sub>2</sub>	19.9	11.7	19.9	12.8
Pt/CeO <sub>2</sub> with EF	15.6	11.9	10.6	8.6

These energy demands for production of hydrogen/syngas should be compared to the combustion energy of the same amount of hydrogen or syngas. In Tables 8 and 9, in the bottom row, these combustion enthalpies are shown. Steam reforming of ethanol was effective for hydrogen and syngas production because the energy demands were much lower than the combustion energy. Industrial production process of hydrogen from methane<sup>46</sup> has a lower energy efficiency, about 63%; it also requires multistep heat exchangers and high-temperature furnace(s). On the other hand, electroforming showed a much higher energy efficiency (i.e., the maximum efficiency was 99% = 143/144 for the Rh catalyst) and can be conducted at very low temperatures, so it does not require a heat exchanger. This novel, simple process showed better or comparable energy efficiency to the industrial catalytic complicated process.

**3.7. Response of the electroforming.** To investigate the response of the electroforming, transient experiments were

**TABLE 8: Electric Energy Demands To Obtain 1 kg Hydrogen by Various Catalytic electroforming Reactions over the Three Catalysts and the Combustion Enthalpy of 1 kg Hydrogen**

temp, K	energy demand, MJ kg-H <sub>2</sub> <sup>-1</sup>			
	EtOH SR	EtOH DC	WGS	CH <sub>4</sub> SR
Pd/CeO <sub>2</sub>	423	118	284	205
	473	56	154	208
	523	66	109	139
Rh/CeO <sub>2</sub>	423	59	568	202
	473	50	489	162
	523	80	229	145
Pt/CeO <sub>2</sub>	423	129	230	139
	473	91	136	114
	523	63	112	132
combustion enthalpy of hydrogen $\Delta H_c/\text{MJ kg}_{\text{H}_2}^{-1}$				143

**TABLE 9: Electric Energy Demands To Obtain 1 kg Syngas (Hydrogen and CO) by Various Catalytic electroforming Reactions over the Three Catalysts, and the Combustion Enthalpy of 1 kg Syngas Having Various Mixture Ratios<sup>a</sup>**

temp, K	energy demand, MJ kg <sub>H<sub>2</sub>+CO</sub> <sup>-1</sup> and H <sub>2</sub> /CO ratio					
	EtOH SR	H <sub>2</sub> /CO	EtOH DC	H <sub>2</sub> /CO	CH <sub>4</sub> SR	H <sub>2</sub> /CO
Pd/CeO <sub>2</sub>	423	24	3.6	44	2.5	146
	473	12	3.7	16	1.7	128
	523	14	3.7	12	1.7	121
Rh/CeO <sub>2</sub>	423	16	5.4	132	4.2	63
	473	13	5.1	114	4.3	80
	523	15	3.2	56	4.5	79
Pt/CeO <sub>2</sub>	423	45	7.4	44	3.3	307
	473	28	6.2	17	2.0	181
	523	18	5.4	14	2.0	254

<sup>a</sup> Combustion enthalpy of syngas (H<sub>2</sub> + CO)  $\Delta H_c$ : 19 MJ kg<sub>H<sub>2</sub>+CO</sub><sup>-1</sup>; 34 MJ kg<sub>3H<sub>2</sub>+CO</sub><sup>-1</sup>; 45 MJ kg<sub>5H<sub>2</sub>+CO</sub><sup>-1</sup>.

conducted to investigate the reaction bed temperature and time-resolved production rates of the products (results are shown in the Supporting Information). The temperature of the catalyst bed was measured by a thermocouple in the reactor tube and an IR thermometer for each reaction mode

of WGS reaction and steam reforming of methane. In mode A without the electric field, the conversion of reactant transited slowly with an increase in the temperature of the catalyst bed. On the other hand, in the case of electroforming, the conversion of the reactant quickly increased with the impressing of the electric field. With the impressing of the electric field, the temperature of the catalyst bed increased up to 35 K. This increase resulted from heat generated by impressing the electric field; heat generated by the reaction itself had little effect on the temperature of the catalyst bed. Conversion of the reactant greatly increased by more than an amount corresponding to the temperature increase in the case of electroforming.

#### 4. Conclusion

We investigated various catalytic reactions in the electroforming system to promote catalytic activity, and we could achieve effective process for hydrogen production. In the presence of the electric field, four reactions proceeded at low temperatures, such as 423 K, where conventional catalytic reaction hardly proceeded. Conversion was greatly increased, and the reaction path was changed to produce much hydrogen. The reaction temperature decreased by at least 150 K by impressing the electric field to the catalyst bed. The WGS reaction and steam reforming of methane were also promoted by impressing the electric field. This electroforming process can produce hydrogen and syngas by using a very small energy demand and has the property of a quick response. Especially for steam reforming of ethanol, hydrogen and syngas can be produced using less energy at low temperatures such as 423 K and at high energy efficiency.

**Supporting Information Available:** Additional information as noted in text. This material is available free of charge via the Internet at <http://pubs.acs.org>.

#### References and Notes

- Bromberg, L.; Cohn, D. R.; Rabinovich, A.; O'Brien, C.; Hochgreb, S. *Energy Fuels* **1998**, *12*, 11.
- Kado, S.; Sekine, Y.; Fujimoto, K. *Chem. Commun.* **1999**, 2485.
- Sekine, Y.; Urasaki, K.; Kado, S.; Matsukata, M.; Kikuchi, E. *Energy Fuels* **2004**, *18*, 455.
- Kado, S.; Sekine, Y.; Nozaki, T.; Okazaki, K. *Catal. Today* **2004**, *89*, 47.
- Liu, C. J.; Marafee, A.; Hill, B.; Xu, G.; Mallinson, R.; Lobban, L. *Ind. Eng. Chem. Res.* **1996**, *35*, 3295.
- Marafee, A.; Liu, C. J.; Xu, G. H.; Mallinson, R.; Lobban, L. *Ind. Eng. Chem. Res.* **1997**, *36*, 632.
- Liu, C. J.; Mallinson, R.; Lobban, L. *J. Catal.* **1998**, *179*, 326.
- Liu, C. J.; Mallinson, R.; Lobban, L. *Appl. Catal., A* **1999**, *178*, 17.
- Thanyachotpaiboon, K.; Chavadej, S.; Caldwell, T. A.; Lobban, L.; Mallinson, R. *AIChE J.* **1998**, *44*, 2252.
- Kado, S.; Urasaki, K.; Nakagawa, H.; Miura, K.; Sekine, Y. *ACS Books Utilization of Green House Gas* **2003**, 852, 303.
- Kado, S.; Sekine, Y.; Urasaki, K.; Okazaki, K.; Nozaki, T. *Stud. Surf. Sci. Catal.* **2004**, *147*, 577.
- Sekine, Y.; Matsukata, M.; Kikuchi, E. *Int. J. Plasma Environ. Sci. Technol.* **2008**, *2*, 72.
- Sekine, Y.; Asai, S.; Kado, S.; Matsukata, M.; Kikuchi, E. *Chem. Eng. Sci.* **2008**, *63*, 5056.
- Iwasaki, Y.; Liu, J.; Zhang, J.; Kitamura, T.; Sakurai, M.; Kameyama, H. *J. Chem. Eng. Jpn.* **2006**, *39*, 216.
- Zhang, Q.; Guo, Y.; Zhou, L.; Sakurai, M.; Kameyama, H. *J. Chem. Eng. Jpn.* **2007**, *40*, 487.
- Zhang, Q.; Sakurai, M.; Kameyama, H. *J. Chem. Eng. Jpn.* **2007**, *40*, 319.
- Oshikawa, Y.; Saito, N.; Inoue, Y. *Surf. Sci.* **1996**, *357/358*, 777.
- Inoue, Y. *Catal. Surv. Jpn.* **1999**, *3*, 95.
- Saito, N.; Sato, Y.; Nishiyama, H.; Inoue, Y. *J. Phys. Chem. C* **2006**, *111*, 1428.
- Sekine, Y.; Tomioka, M.; Matsukata, M.; Kikuchi, E. *Catal. Today*, in press. doi:10.1016/j.cattod.2009.03.027.
- Haga, F.; Nakajima, T.; Miya, H.; Mishima, S. *Catal. Lett.* **1997**, *48*, 223.
- Cavallaro, S. *Energy Fuels* **2000**, *14*, 1195.
- Galvita, V. V.; Semin, G. L.; Belyaev, V. D.; Semikolenov, V. A.; Tsiakaras, P.; Sobyenin, V. A. *Appl. Catal., A* **2001**, *220*, 123.
- Marino, F.; Boveri, M.; Baronetti, G.; Laborde, M. *Int. J. Hydrogen Energy* **2001**, *26*, 665.
- Klouz, V.; Fierro, V.; Denton, P.; Katz, H.; Lisse, J. P.; Bouvot-Mauduit, S.; Mirodatos, C. *J. Power Sources* **2002**, *105*, 26.
- Breen, J. P.; Burch, R.; Coleman, H. M. *Appl. Catal., B* **2002**, *39*, 65.
- Diagne, C.; Idriss, H.; Kiennemann, A. *Catal. Commun.* **2002**, *3*, 565.
- Fatsikostas, A. N.; Kondarides, D. I.; Verykios, X. E. *Catal. Today* **2002**, *75*, 145.
- Srinivas, D.; Satyanarayana, C. V. V.; Potdar, H. S.; Ratnasamy, P. *Appl. Catal., A* **2003**, *246*, 323.
- Batista, M. S.; Santos, R. K. S.; Assaf, E. M.; Assaf, J. M.; Ticianelli, E. A. *J. Power Sources* **2003**, *124*, 99.
- Freni, S.; Cavallaro, S.; Mondello, N.; Spadaro, L.; Frusteri, F. *Catal. Commun.* **2003**, *4*, 259.
- Liguras, D. K.; Kondarides, D. I.; Verykios, X. E. *Appl. Catal., B* **2003**, *43*, 345.
- Fatsikostas, A. N.; Verykios, X. E. *J. Catal.* **2004**, *225*, 439.
- Frusteri, F.; Freni, S.; Spadaro, L.; Chiodo, V.; Bonura, G.; Donato, S.; Cavallaro, S. *Catal. Commun.* **2004**, *5*, 611.
- Llorca, J.; Homs, N.; Sales, J.; Fierro, J. L. G.; de la Piscina, P. R. *J. Catal.* **2004**, *222*, 470.
- Haryanto, A.; Fernando, S.; Murali, N.; Adhikari, S. *Energy Fuels* **2005**, *19*, 2098.
- Kugai, J.; Velu, S.; Song, C. S. *Catal. Lett.* **2005**, *101*, 255.
- Meng, N.; Dennis, Y. L.; Michael, K. H. L. *Int. J. Hydrogen Energy* **2007**, *32*, 3238.
- Urasaki, K.; Fukuda, Y.; Sekine, Y.; Matsukata, M.; Kikuchi, E. *J. Jpn. Pet. Inst.* **2008**, *51*, 83.
- Urasaki, K.; Tokunaga, K.; Sekine, Y.; Matsukata, M.; Kikuchi, E. *Catal. Commun.* **2008**, *9*, 600.
- Basagiannis, A. C.; Panagiotopoulou, P.; Verykios, X. E. *Top. Catal.* **2008**, *51*, 2.
- Yamazaki, O.; Tomishige, K.; Fujimoto, K. *Appl. Catal., A* **1996**, *136*, 49.
- Li, B.; Watanabe, R.; Maruyama, K.; Kunimori, K.; Tomishige, K. *Catal. Today* **2005**, *104*, 7.
- Mukainakano, Y.; Li, B.; Kado, S.; Miyazawa, T.; Okumura, K.; Miyao, T.; Naito, S.; Kunimori, K.; Tomishige, K. *Appl. Catal., A* **2007**, *318*, 252.
- Rostrup-Nielsen, J. R. *Phys. Chem. Chem. Phys.* **2001**, *3*, 283.
- Rostrup-Nielsen, J. R. *Catal. Today* **2006**, *111*, 4.
- Wei, J.; Iglesia, E. *J. Phys. Chem. B* **2004**, *108*, 4094.
- Wei, J.; Iglesia, E. *J. Phys. Chem. B* **2004**, *108*, 7253.
- Wei, J.; Iglesia, E. *J. Catal.* **2004**, *225*, 116.
- Wei, J.; Iglesia, E. *Angew. Chem.* **2004**, *43*, 3685.
- Wei, J.; Iglesia, E. *J. Catal.* **2004**, *224*, 370.
- Urasaki, K.; Sekine, Y.; Kawabe, S.; Kikuchi, E.; Matsukata, M. *Appl. Catal., A* **2005**, *286*, 23.
- Hayakawa, T.; Suzuki, S.; Nakamura, J.; Uchijima, T.; Hamakawa, S.; Suzuki, K.; Shishido, T.; Takehira, K. *Appl. Catal., A* **1999**, *183*, 273.
- Tsyganok, A. I.; Tsunoda, T.; Hamakawa, S.; Suzuki, K.; Takehira, K.; Hayakawa, T. *J. Catal.* **2003**, *213*, 191.
- Shido, T.; Iwasawa, Y. *J. Catal.* **1991**, *129*, 343.
- Shido, T.; Iwasawa, Y. *J. Catal.* **1992**, *136*, 493.
- Shido, T.; Iwasawa, Y. *J. Catal.* **1993**, *141*, 71.
- Bunluesin, T.; Gorte, R. J.; Graham, G. W. *Appl. Catal., B* **1998**, *15*, 107.
- Hilaire, S.; Wang, X.; Luo, T.; Gorte, R. J.; Wagner, J. *Appl. Catal., A* **2001**, *215*, 271.
- Peña, M. A.; Fierro, L. G. *Chem. Rev.* **2001**, *101*, 1981.
- Jacobs, G.; Williams, L.; Graham, U.; Thomas, G. A.; Sparks, D. E.; Davis, B. H. *Appl. Catal., A* **2003**, *252*, 107.
- Tanaka, Y.; Utaka, T.; Kikuchi, R.; Takeguchi, T.; Sasaki, K.; Eguchi, K. *J. Catal.* **2003**, *215*, 271.
- Tanaka, Y.; Utaka, T.; Kikuchi, R.; Sasaki, K.; Eguchi, K. *Appl. Catal., A* **2003**, *242*, 287.
- Giroux, T.; Hwang, S.; Ruettinger, Y.; Shore, L. *Appl. Catal., B* **2005**, *56*, 95.
- Tanaka, Y.; Takeguchi, T.; Kikuchi, R.; Eguchi, K. *Appl. Catal., A* **2005**, *279*, 59.
- Shishido, T.; Yamamoto, M.; Li, D.; Tian, Y.; Morioka, H.; Honda, M.; Sano, T.; Takehira, K. *Appl. Catal., A* **2006**, *303*, 62.

- (67) Jacobs, G.; Ricote, S.; Davis, B. H. *Appl. Catal., A* **2006**, *302*, 14.  
(68) Sato, Y.; Soma, Y.; Miyao, T.; Naito, S. *Appl. Catal., A* **2006**, *304*, 78.  
(69) Sato, Y.; Terada, K.; Soma, Y.; Miyao, T.; Naito, S. *Catal. Commun.* **2006**, *7*, 91.  
(70) Iida, H.; Igarashi, A. *Appl. Catal., A* **2006**, *303*, 48.  
(71) Iida, H.; Igarashi, A. *Appl. Catal., A* **2006**, *303*, 192.  
(72) Iida, H.; Igarashi, A. *Appl. Catal., A* **2006**, *298*, 152.  
(73) Atake, I.; Nisida, K.; Li, D.; Shishido, T.; Oumi, Y.; Sano, T.; Takehira, K. *J. Mol. Catal., A* **2007**, *275*, 130.  
(74) Jacobs, G.; Davis, B. H. *Appl. Catal., A* **2007**, *333*, 192.  
(75) Sekine, Y.; Takamatsu, H.; Aramaki, S.; Ichishima, K.; Takada, M.; Matsukata, M.; Kikuchi, E. *Appl. Catal., A* **2009**, *352*, 214.

JP906137H